

Charged Higgs Pair Production at the LHC as a Probe of the Top-Seesaw Assisted Technicolor Model

Guo-Li Liu^{1*}, Xiao-Fei Guo¹, Kun Wu¹, Ji Jiang¹, Ping Zhou^{1,2}

¹ *Department of Physics, Zhengzhou University, Zhengzhou, 450001, China*

² *National Space Science Center, Chinese Academy of Science, 100190*

Abstract

The top-seesaw assisted technicolor (TC) model, which was proposed recently to explain the 126 GeV Higgs mass discovered by the Large Hadron Colliders (LHC), predicts light and heavy charged Higgs bosons in addition to the neutral Higgses. In this paper we will study the pair productions of the charged Higgs, proceeding through gluon-gluon fusion and quark-anti-quark annihilation, at the LHC in the frame of the top-seesaw assisted TC model. We find that in a large part of parameter space the production cross sections of the light charged Higgs pair at the LHC can be quite large compared with the low standard model backgrounds, while it is impossible for the pair production of the heavy ones to be detected with the strong final mass suppression. Therefore, at the LHC future experiments, the light charged Higgs pair production may be served as a probe of this new TC model.

PACS numbers: 12.60.Nz, 14.80.Bn

* guoliliu@zzu.edu.cn

I. INTRODUCTION

Though it is successfully tested by various high energy experiments, including the 126 GeV Higgs [1] discovery by the Large Hadron Collider (LHC) in CERN [2], the standard model (SM) of particle physics [3] is still believed by many people to be an effective theory below certain high energy scale. The origin of the mechanism for electroweak symmetry breaking(EWSB) as well as the Yukawa couplings remain a mystery in current particle physics. Besides, the neutrino oscillation experiments indicate that neutrinos are massive, which manifestly requires new physics beyond the standard model [4]. At the same time, SM itself cannot provide viable dark matter candidates [5]. Therefore, it is interesting from both the theoretical point of view and the experimental search aspects to extend the standard model to understand the EWSB mechanism and possibly extended the Higgs sector.

The TC-type models[6, 7], in which EWSB can be achieved via introducing the new strong interaction– the TC interaction, without the aid of the elementary scalar Higgs boson [8–13], could completely avoid the problems arising from the elementary Higgs scalar field in the SM. The TC models open up new possibilities for new physics beyond the SM, and might produce observed signatures in future high energy collider experiments.

Among various kinds of TC theories, the topcolor scenario[14] is attractive because it can not only provide a possible dynamical EWSB mechanism, but explain the large top quark mass simultaneously. These traditional TC theories, however, have encountered a severe obstruction since they are difficult to provide a light scalar candidate. To solve the problem, top-seesaw assisted TC model[12, 15] is proposed, which requires EWSB are shared between different contributions, i.e. there exists different scalars, with different value expectation values (VEVs), say v_1 and v_2 , satisfying $v_{EW}^2 = v_1^2 + v_2^2$, with $v_1(v_2) < v_{EW}$, the electroweak scale. Then the masses of the excitations in different sections, which are dictated by v_1 and v_2 , may also be smaller than v_{EW} .

With the enlarged gauge group, the top-seesaw assisted TC model predicts more Higgs bosons, including the additional charged scalars. Actually, the existence of new charged scalars are predicted in many new physics theories, such as the supersymmetry[16], TC (topcolor)[6, 7, 14], little Higgs[17] and the left-right twin Higgs[18], etc. These charged new scalars may have very large signals at the colliders, and If we can find any evidence of them, it would necessarily be the signal of the new physics beyond the SM. Thus, studying the

signals of the charged scalars[19] at the running LHC will be of special interest.

As we know, the pair productions of the charged scalars, at the tree-level or the one-loop level, may have very large production rates [20], so in the top-seesaw assisted TC model, we can consider the pair production of the new charged scalars at the LHC, and analysis the observable possibility, which may serve as a good channel to probe such new TC model.

In this paper, we will study how the top-seesaw assisted TC model constrains the scalar pair production processes $gg \rightarrow S^+S^-$ and $q\bar{q} \rightarrow S^+S^-$ (S^\pm denotes the charged scalars and $q = u, d, c, s, b$ quarks). We will calculate the cross sections of these processes and compare the signals with their SM backgrounds.

In Sec. II, the newly proposed TC model relative to our calculations is reviewed and the new couplings related to the scalar pair production processes $gg \rightarrow S^+S^-$ and $q\bar{q} \rightarrow S^+S^-$ ($q = u, d, c, s, b$ quarks) at the LHC are also given in this section. Sec. III shows the numerical results of these processes and analysis simply the SM backgrounds and the detectable probability of the final state at the the LHC. Our summary and discussions are given in Sec. IV.

II. THE TOP-SEESAW ASSISTED TC MODEL AND THE RELEVANT COUPLINGS

To solve the phenomenological difficulties of traditional TC theory, the top-seesaw assisted TC model[15] was proposed by adding new vector-like quarks in the TC models. The basic idea of the models is to combine top-seesaw model[8, 9, 11–13] with TC model[6] in a way similar to topcolor assisted TC (TC2)[7] models. In this new model, masses of all leptons and the light quarks are assumed to be generated by some underlying ETC dynamics operating at much higher scales and the mass patterns of the third and fourth quark generations are mainly provided dynamically by the seesaw mechanism.

A. The low energy effective lagrangian of the top-seesaw assisted model

The underlying gauge symmetry in the ultraviolet (UV) part of top-seesaw theory is $SU(3)_1 \times SU(3)_2 \times SU(2)_L \times U(1)_1 \times U(1)_2$, which is broken to $SU(3)_{QCD} \times SU(2)_L \times U(1)_Y$, generating $8 + 1$ massive gauge bosons G' and Z' , which masses are assumed at the same

order, denoted as M_V . At low energies, the interactions via the $8 + 1$ massive gauge bosons exchange lead to effective four fermion interactions, of which the terms that interest us are given as

$$\mathcal{L}_S^{4f} = G_b \left(\bar{D}_R^{(4)} Q_L^{(3)} \right)^2 + G_t \left(\bar{U}_R^{(4)} Q_L^{(3)} \right)^2 + G_{tb} \left(\bar{Q}_L^{(3)} U_R^{(4)} \right) \left(\bar{D}_R^{(4)c} i\tau_2 Q_L^{(3)c} \right) + h.c., \quad (1)$$

where $G_{t,b}$ are the scalar mass terms and G_{tb} are the diagonal terms and we here will not discuss them in detail, since every coupling that we will obtain is actually closely related to the specific form of different fields, which will be discussed later.

In this section, we will consider the low energy effective Lagrangian for the four fermion interaction sector and its mixing with the TC sector, of which, the dynamical top seesaw sector based on the conventional Nambu-Jona-Lasinio (NJL) model [21], can be given by the fermion bubble sum approximation [12, 22], The low energy effective Lagrangian valid for $\mu < \Lambda \simeq M'_G \simeq M'_Z$, where μ is the scale of the theory after the gauge breaking $SU(3)_1 \times SU(3)_2 \times U(1)_1 \times U(1)_2 \rightarrow SU(3)_{\text{QCD}} \times U(1)_Y$ and Λ is ultraviolet (UV) cutoff.

The auxiliary Higgs fields $\Phi_{1,2}$ are introduced with $\Phi_1 \sim \bar{D}_R^{(4)} Q_L^{(3)}$ and $\Phi_2 \sim \bar{U}_R^{(4)} Q_L^{(3)}$, and $\Phi_{1,2}$ ($i = 1, 2$) can be further parameterized as,

$$\Phi_i = \begin{pmatrix} \pi_i^+ \\ \frac{1}{\sqrt{2}}[v_i + h_i^0 - i\pi_i^0] \end{pmatrix}. \quad (2)$$

As we know, the top-seesaw assisted TC model includes two sections, where one sector, i.e, the top seesaw section, generates the large top quark mass and partially contributes to EWSB while the other sector, i.e, TC interaction, is responsible for the bulk of EWSB and the generation of light fermion masses. The Nambu-Goldstone bosons (NGBs) in the TC sector can be described as the most minimal electroweak chiral Lagrangian[23] according to the the most minimal structure breaking $G/H = [SU(2)_L \times SU(2)_R/SU(2)_V]$, so the leading order chiral Lagrangian can be written as

$$\mathcal{L}_{\text{EWCL}}^{(2)} = |D_\mu \Phi_{\text{TC}}|^2, \quad \text{with} \quad \Phi_{\text{TC}} = \begin{pmatrix} \pi_{\text{TC}}^+ \\ \frac{1}{\sqrt{2}}[v_{\text{TC}} - i\pi_{\text{TC}}^0] \end{pmatrix}, \quad (3)$$

where $\tilde{\Phi}_{\text{TC}} \equiv i\tau^2 \Phi_{\text{TC}}^*$. The covariant derivative $D_\mu \Phi_{\text{TC}}$ is

$$D_\mu \Phi_{\text{TC}} = \partial_\mu \Phi_{\text{TC}} - ig W_\mu^a T^a \Phi_{\text{TC}} - \frac{1}{2} g' B_\mu \Phi_{\text{TC}}, \quad (4)$$

where $T^a = (1/2)\tau^a$, and g and g' are gauge couplings of the SM $SU(2)_L, U(1)_Y$ gauge boson fields W_μ, B_μ , respectively.

The reason for the missing CP-even component of the Φ_{TC} in Eq.(3), is that, the Higgs effects are found to be small [23], since the Nambu-Goldstone bosons (NGBs) in the TC sector, which are described by the most minimal structure of the electroweak chiral Lagrangian[23], can be a strongly interacting heavy-Higgs-boson sector, i.e., the gauged nonlinear σ model, i.e., the nonrenormalizability of the no-Higgs-boson theory. And furthermore, we have also assumed that the TC section only provides the very small masses of the light fermions in a higher scale, so the effects of the "Higgs" from TC sector at low energy are negligible, compared to those of the top-seesaw sector. Actually, in this model we will set $m_{ETC} = \Lambda_{TC} = 4\pi v_{TC}$ corresponding to the cutoff scale for the non-linear sigma model which we use to describe the TC sector [15].

At the low energy, the effective Lagrangian concerning Higgs section in the top-seesaw assisted TC model can be explicitly written by

$$\mathcal{L}_{\text{higgs}}(\Phi_1, \Phi_2, \Phi_{TC}) = \sum_{i=1,2,TC} |D_\mu \Phi_i|^2 + \mathcal{L}_{\text{yukawa}} - V(\Phi_1, \Phi_2, \Phi_{TC}). \quad (5)$$

where the covariant derivatives of Φ_i are the same forms as that in Eq.(4) and the effective Yukawa interaction terms $\mathcal{L}_{\text{yukawa}}$ are

$$\begin{aligned} \mathcal{L}_{\text{yukawa}} = & - \sum_{i,j=1,2,3}^{\text{quarks}} y_{ij}^{(d)} \bar{Q}_L^{(i)} \Phi_{TC} D_R^{(j)} - \sum_{i,j=1,2,3}^{\text{quarks}} y_{ij}^{(u)} \bar{Q}_L^{(i)} \tilde{\Phi}_{TC} U_R^{(j)} \\ & - y_1 \bar{Q}_L^{(3)} \Phi_1 D_R^{(4)} - y_2 \bar{Q}_L^{(3)} \tilde{\Phi}_2 U_R^{(4)} + \text{h.c.}, \end{aligned} \quad (6)$$

where the Yukawa couplings $y_{1,2}$ and y_{ij} in the above equation are given later, when discussing the Yukawa terms of the 3, 4 generations.

The potential $V(\Phi_1, \Phi_2, \Phi_{TC})$ in Eq.(5) can be defined as two sections

$$V(\Phi_1, \Phi_2, \Phi_{TC}) = V_{\text{TSS}}(\Phi_1, \Phi_2) + V_M(\Phi_1, \Phi_2, \Phi_{TC}). \quad (7)$$

Similar to the attainment of the Yukawa terms in Eq. (6), the former part of the above Higgs potential can be given as,

$$\begin{aligned} V_{\text{TSS}}(\Phi_1, \Phi_2) = & M_{11}^2 |\Phi_1|^2 + M_{22}^2 |\Phi_2|^2 - M_{12}^2 [\Phi_1^\dagger \Phi_2 + \text{h.c.}] \\ & + \frac{1}{2} \lambda_1 (\Phi_1^\dagger \Phi_1)^2 + \frac{1}{2} \lambda_2 (\Phi_2^\dagger \Phi_2)^2 + \lambda_3 (\Phi_1^\dagger \Phi_1) (\Phi_2^\dagger \Phi_2) + \lambda_4 (\Phi_1^\dagger \Phi_2) (\Phi_2^\dagger \Phi_1), \end{aligned} \quad (8)$$

where M_{ij}^2 ($i, j = 1, 2$) are the Higgs mass terms and $\lambda_{1,2,3,4}$, Higgs quartic couplings. M_{ij}^2 ($i, j = 1, 2$) can be confined by the scalar masses, while $\lambda_{1,2,3,4}$ can be constrained by solving the RGEs with the compositeness conditions[22, 24] of this model, and we take $\lambda_1 = \lambda_1 = \lambda_1 = \lambda_1 = 1$ in this paper, since they are in the order of $\mathcal{O}(1)$ [15].

Different from the obtainment of the Yukawa terms and the potential $V_{TSS}(\Phi_1, \Phi_2)$, which are both arising from the underlying theory of the four fermion interactions in Eq.(1), the terms $V_M(\Phi_1, \Phi_2, \Phi_{TC})$, which are the mixing between the TC sector and the top-seesaw sector [25], can be written as

$$V_M(\Phi_1, \Phi_2, \Phi_{TC}) = c_1 v_1^2 \left| \Phi_1 - \frac{v_1}{v_{TC}} \Phi_{TC} \right|^2 + c_2 v_2^2 \left| \Phi_2 - \frac{v_2}{v_{TC}} \Phi_{TC} \right|^2, \quad (9)$$

where $c_{1,2}$ are dimensionless parameters of $\mathcal{O}(\infty)$ and we will take $c_1 = c_2 = 1$ in our calculations.

Under the above definitive scalars, we know that the vacuum structure of this model is determined by three vacuum expectation values (VEVs) of the three scalar doublets, $v_{TC,1,2}$, which all contribute to EWSB and satisfy the relation $v_1^2 + v_2^2 + v_{TC}^2 = v_{EW}^2$ with $v_{EW} = 246 \text{ GeV}$. Mixing angles β and ϕ are introduced with the definition as

$$\tan \beta \equiv \frac{v_2}{v_1}, \quad \tan^2 \phi \equiv \frac{v_{TC}^2}{v_1^2 + v_2^2}, \quad (10)$$

$$\text{or } v_{TC} = v_{EW} \sin \phi, \quad v_1 = v_{EW} \cos \phi \cos \beta, \quad v_2 = v_{EW} \cos \phi \sin \beta.$$

B. The Higgs boson spectrum in the present model

From the scalar doublets shown in Eq.(2) and Eq.(3), we know that there should be 11 scalars, three of which, however, will become the longitudinal components of the electroweak bosons, in the proper parameterization form, so there should be 8 scalars left. Since 1 CP-odd neutral and 2 charged bosons will be "eaten", there should exist 2 CP-odd, 2 CP-even, 4 charged Higgs. In the following, we will consider the mixing and coupling with the other particles concerned in this paper.

We can write down the quadratic terms of the NGB fields via the potentials $V_{TSS}(\Phi_1, \Phi_2)$ and $V_M(\Phi_1, \Phi_2, \Phi_{TC})$ in Eq.(8) and Eq.(9) as

$$\mathcal{L}^{\text{qd}} = -\frac{1}{2}(\pi_1^0 \ \pi_2^0 \ \pi_{TC}^0) \mathcal{M}_\pi^2 \begin{pmatrix} \pi_1^0 \\ \pi_2^0 \\ \pi_{TC}^0 \end{pmatrix} - (\pi_1^+ \ \pi_2^+ \ \pi_{TC}^+) \mathcal{M}_{\pi^\pm}^2 \begin{pmatrix} \pi_1^- \\ \pi_2^- \\ \pi_{TC}^- \end{pmatrix} - \frac{1}{2}(h_1^0 \ h_2^0) \mathcal{M}_h^2 \begin{pmatrix} h_1^0 \\ h_2^0 \end{pmatrix} \quad (11)$$

The mass matrix of the charged Higgs sector is,

$$\mathcal{M}_{\pi\pm}^2|_{\text{TC}=0} = \left[M_{12}^2 - \frac{1}{2} \lambda_4 v_{\text{EW}}^2 \cos^2 \phi \sin \beta \cos \beta \right] \begin{pmatrix} \tan \beta & -1 \\ -1 & \tan \beta \end{pmatrix}, \quad (12)$$

where M_{12}^2 can be treated as the free parameters.

Due to the mixing of the top-seesaw and TC sectors, the mass matrix of the charged CP-odd Higgs boson fields, $\pi_i^\pm (i = 1, 2, \text{TC})$, can be given as

$$\mathcal{M}_{\pi\pm}^2 = \left(\begin{array}{cc|c} \mathcal{M}_{\pi\pm}^2|_{\text{TC}=0} & & 0 \\ & & 0 \\ \hline 0 & 0 & 0 \end{array} \right) + \begin{pmatrix} c_1 v_1^2 & 0 & -M_1^2 \\ 0 & c_2 v_2^2 & -M_2^2 \\ -M_1^2 & -M_2^2 & M_1^2 \cos \beta \cot \phi + M_2^2 \sin \beta \cot \phi \end{pmatrix}. \quad (13)$$

where $c_1(c_2)$ is a dimensionless parameter and $M_1^2 = c_1 v_1^2 \frac{v_1}{v_{\text{TC}}}$, $M_2^2 = c_2 v_2^2 \frac{v_2}{v_{\text{TC}}}$.

In terms of the mass basis, the CP-odd neutral Higgs bosons and the charged Higgs bosons can be given as

$$\begin{pmatrix} G^0 \\ A_2^0 \\ A_1^0 \end{pmatrix} = O_0^T \begin{pmatrix} \pi_1^0 \\ \pi_2^0 \\ \pi_{\text{TC}}^0 \end{pmatrix}, \quad \begin{pmatrix} G^\pm \\ H_2^\pm \\ H_1^\pm \end{pmatrix} = \mathcal{O}_\pm^T \begin{pmatrix} \pi_1^\pm \\ \pi_2^\pm \\ \pi_{\text{TC}}^\pm \end{pmatrix}, \quad (14)$$

with the orthogonal matrix O_p ($p = 0, \pm$) as [27]

$$O_p = \begin{pmatrix} \cos \phi \cos \beta & -\sin \beta \cos \zeta_p + \sin \phi \cos \beta \sin \zeta_p & -\sin \beta \sin \zeta_p - \sin \phi \cos \beta \cos \zeta_p \\ \cos \phi \sin \beta & \cos \beta \cos \zeta_p + \sin \phi \sin \beta \sin \zeta_p & \cos \beta \sin \zeta_p - \sin \phi \sin \beta \cos \zeta_p \\ \sin \phi & -\cos \phi \sin \zeta_p & \cos \phi \cos \zeta_p \end{pmatrix}. \quad (15)$$

Here the mixing angle between the mass and interaction eigenstates $\tan \zeta_p$ is composed as

$$\tan \zeta_p = \frac{\hat{M}_{S_2}^2 \cos \phi \sin \phi - (M_1^2 \cos \beta + M_2^2 \sin \beta)}{\sin \phi (M_1^2 \sin \beta - M_2^2 \cos \beta)}. \quad (16)$$

C. The couplings of the charged Higgs boson to the third and the fourth generation quarks

We will discuss the mixing between the third generation quarks and their vector-like partners, i.e., the fourth quarks. Firstly we find the fermion mass part after the dynamical

EWSB,

$$- \begin{pmatrix} \bar{U}_L^{(3)} & \bar{U}_L^{(4)} \end{pmatrix} \begin{pmatrix} 0 & \Sigma_U \\ M_U^{(43)} & M_U^{(44)} \end{pmatrix} \begin{pmatrix} U_R^{(3)} \\ U_R^{(4)} \end{pmatrix} - \begin{pmatrix} \bar{D}_L^{(3)} & \bar{D}_L^{(4)} \end{pmatrix} \begin{pmatrix} 0 & \Sigma_D \\ M_D^{(43)} & M_D^{(44)} \end{pmatrix} \begin{pmatrix} D_R^{(3)} \\ D_R^{(4)} \end{pmatrix} + \text{h.c.} \quad (17)$$

Now, the quark mixing matrices U, D was presented to reflect the seesaw mechanism for the third and the fourth generation, and the quark mixing matrices are given as [15]

$$U_{\alpha\beta}^L \simeq \begin{pmatrix} 1 & 0 & 0 & 0 \\ 0 & 1 & 0 & 0 \\ 0 & 0 & c_L^t & s_L^t \\ 0 & 0 & -s_L^t & c_L^t \end{pmatrix}, \quad U_{\alpha\beta}^R \simeq \begin{pmatrix} 1 & 0 & 0 & 0 \\ 0 & 1 & 0 & 0 \\ 0 & 0 & -c_R^t & s_R^t \\ 0 & 0 & s_R^t & c_R^t \end{pmatrix}, \quad (18)$$

$$D_{\alpha\beta}^L = U_{\alpha\beta}^L |_{t \rightarrow b}, \quad D_{\alpha\beta}^R = U_{\alpha\beta}^R |_{t \rightarrow b}. \quad (19)$$

where $c_L^t \equiv \cos \theta_L^t$, $s_L^t \equiv \sin \theta_L^t$, etc. These fermion mixing matrices U and D in the above two equations diagonalize the mass mixing matrices in Eq.(17), and the eigenvalues of them are $m_{t,b}(TSS)$ (masses of top and bottom quarks generating by top-seesaw), and $m_{T,B}$ (mass of the vector-like partner of the third generation quark), with $m_{T,B} > m_{t,b}(TSS)$. So $c_L^{t,b}, s_L^{t,b}$ can be written as

$$[c_L^t]^2 \equiv \frac{m_T^2 - \Sigma_U^2}{m_T^2 - m_t^2(TSS)}, \quad [s_L^t]^2 \equiv \frac{m_t^2(TSS)}{\Sigma_U^2} [c_L^t]^2, \quad (20)$$

$$[c_L^b]^2 \equiv \frac{m_B^2 - \Sigma_D^2}{m_B^2 - m_b^2(TSS)}, \quad [s_L^b]^2 \equiv \frac{m_b^2(TSS)}{\Sigma_D^2} [c_L^b]^2. \quad (21)$$

In this model, the Yukawa terms for third generation quarks and their vector-like partners, i.e., the fourth quarks, which is a part of Eq.(6), are written explicitly as

$$\mathcal{L}_{\text{yukawa}}^{3-4} = -y_1 \bar{Q}_L^{(3)} \Phi_1 D_R^{(4)} - y_2 \bar{Q}_L^{(3)} \tilde{\Phi}_2 U_R^{(4)} - y_{\text{TC}}^b \bar{q}_L \Phi_{\text{TC}} b_R - y_{\text{TC}}^t \bar{q}_L \tilde{\Phi}_{\text{TC}} t_R + \text{h.c.}, \quad (22)$$

where the couplings $y^{1,2}$ and $y_{\text{TC}}^{b,t}$ are given by[15]

$$y_1 = \frac{\sqrt{2}\Sigma_D}{v_1}, \quad y_2 = \frac{\sqrt{2}\Sigma_U}{v_2}, \quad y_{\text{TC}}^b = \frac{\sqrt{2}\epsilon_b m_b}{v_{\text{TC}}}, \quad y_{\text{TC}}^t = \frac{\sqrt{2}\epsilon_t m_t}{v_{\text{TC}}}, \quad (23)$$

Note that $y_{1,2}$ is obtained via the renormalization group equations (RGEs) and according to the discussion in Ref. [15], $y_1 = y_2 = 2$ is appropriate. From the definitions of $y_{\text{TC}}^{b,t}$ and the couplings in Eq.(22) we can see clearly that the parameters ϵ_t and ϵ_b are the fraction of the ETC interactions to the masses of the top and bottom quarks, respectively. In order to

realize the top-seesaw dynamics, we must have $\Sigma_U > m_t(TSS) = (1 - \epsilon_t)m_t$ with $\epsilon_t < 0.1$, so we can take Σ_U as a free parameter only if the seesaw condition mentioned above is satisfied.

Taking the Eq.(14) and Eq.(18) into Eq.(22), by which the charged Higgs and the quarks are changed into mass eigenstates, we can obtain the couplings of the charged Higgs to the heavy quarks,

$$\begin{aligned}\mathcal{L}_{Hff'} = & (a_{tb}^L + b_{tb}^L \gamma^5) H_L^+ \bar{t} b + (a_{tb}^H + b_{tb}^H \gamma^5) H_H^+ \bar{t} b + (a_{Tb}^L + b_{Tb}^L \gamma^5) H_L^+ \bar{T} b + (a_{Tb}^H + b_{Tb}^H \gamma^5) H_H^+ \bar{T} b \\ & + (a_{tB}^L + b_{tB}^L \gamma^5) H_L^+ \bar{t} B + (a_{tB}^H + b_{tB}^H \gamma^5) H_H^+ \bar{t} B + (a_{TB}^L + b_{TB}^L \gamma^5) H_L^+ \bar{T} B \\ & + (a_{TB}^H + b_{TB}^H \gamma^5) H_H^+ \bar{T} B + h.c.\end{aligned}\quad (24)$$

where

$$a_{tb}^L = \frac{1}{2}(-y_1 c_L^t s_R^b O_{21} + y_2 s_R^t c_L^b O_{22} - y_{TC}^b O_{23} + y_{TC}^t O_{23}), \quad (25)$$

$$a_{tB}^L = \frac{1}{2}(-y_1 c_L^t c_R^b O_{21} - y_2 s_L^b s_R^t O_{22}), \quad (26)$$

$$a_{Tb}^L = \frac{1}{2}(y_1 s_L^t s_R^b O_{21} + y_2 c_R^t c_L^b O_{22}), \quad (27)$$

$$a_{TB}^L = \frac{1}{2}(y_1 s_L^t c_R^b O_{21} - y_2 c_R^t s_L^b O_{22}), \quad (28)$$

$$b_{q_i q_j}^L = a_{q_i q_j}^L |_{y_2 \rightarrow -y_2, y_{TC}^t \rightarrow -y_{TC}^t}; \quad a_{q_i q_j}^H (b_{q_i q_j}^H) = a_{q_i q_j}^L (b_{q_i q_j}^L) |_{O_{2i} \rightarrow O_{3i}}; \quad (29)$$

with $q_i, q_j = t, b, T, B$ ($i \neq j$) quarks.

D. The couplings of the charged Higgs boson pair to neutral Higgs

Diagonalizing the fermions and scalars in the the Higgs mixing potential V_M in Eq.(5), which are related to three scalars couplings, we can arrive in the three scalars couplings as,

$$\mathcal{L}_{scc} = Y_{hcc}^L h^0 H_L^+ H_L^- + Y_{Hcc}^L H^0 H_L^+ H_L^- + Y_{hcc}^H h^0 H_H^+ H_H^- + Y_{Hcc}^H H^0 H_H^+ H_H^- \quad (30)$$

Where

$$\begin{aligned}Y_{hcc}^L &= -\lambda_1 v_1 s_\alpha (O_p^-)_{13}^2 + \lambda_2 v_2 c_\alpha (O_p^-)_{23}^2 - \lambda_3 v_1 s_\alpha (O_p^-)_{23}^2 + \lambda_3 v_2 c_\alpha (O_p^-)_{13}^2 + \lambda_4 c_h (O_p^-)_{23} (O_p^-)_{13}, \\ Y_{Hcc}^L &= \lambda_1 v_1 c_\alpha (O_p^-)_{13}^2 + \lambda_2 v_2 s_\alpha (O_p^-)_{23}^2 + \lambda_3 v_1 c_\alpha (O_p^-)_{23}^2 + \lambda_3 v_2 s_\alpha (O_p^-)_{13}^2 + \lambda_4 c_H (O_p^-)_{23} (O_p^-)_{13}, \\ Y_{hcc}^H &= -\lambda_1 v_1 s_\alpha (O_p^-)_{12}^2 + \lambda_2 v_2 c_\alpha (O_p^-)_{22}^2 - \lambda_3 v_1 s_\alpha (O_p^-)_{22}^2 + \lambda_3 v_2 c_\alpha (O_p^-)_{12}^2 + \lambda_4 c_h (O_p^-)_{23} (O_p^-)_{12}, \\ Y_{Hcc}^H &= \lambda_1 v_1 c_\alpha (O_p^-)_{12}^2 + \lambda_2 v_2 s_\alpha (O_p^-)_{22}^2 + \lambda_3 v_1 c_\alpha (O_p^-)_{22}^2 + \lambda_3 v_2 s_\alpha (O_p^-)_{12}^2 + \lambda_4 c_H (O_p^-)_{23} (O_p^-)_{12}.\end{aligned}\quad (31)$$

Here $s_\alpha = \sin \alpha$, $c_\alpha = \cos \alpha$, and α is the neutral Higgs mixing, with

$$\begin{pmatrix} H^0 \\ h^0 \end{pmatrix} = \begin{pmatrix} \cos \alpha & \sin \alpha \\ -\sin \alpha & \cos \alpha \end{pmatrix} \begin{pmatrix} h_1^0 \\ h_2^0 \end{pmatrix}. \quad (32)$$

The matrix O_p^- is the inverse of the psedu-Goldstone boson mixing matrix of O_p shown in Eq.(15), which can be given as

$$O_p^- = \begin{pmatrix} \cos \phi \cos \beta & -\cos \zeta_p \sin \beta + \cos \beta \sin \phi \sin \zeta_p & -\cos \beta \cos \zeta_p \sin \phi - \sin \beta \sin \zeta_p \\ \cos \phi \sin \beta & \cos \beta \cos \zeta_p + \sin \phi \sin \beta \sin \zeta_p & -\cos \zeta_p \sin \phi \sin \beta + \cos \beta \sin \zeta_p \\ \sin \phi & -\cos \phi \sin \zeta_p & \cos \phi \cos \zeta_p \end{pmatrix}. \quad (33)$$

The coupling constants c_h and c_H are written as,

$$c_H = v_1 s_\alpha + v_2 c_\alpha, \quad c_h = v_1 c_\alpha - v_2 s_\alpha \quad (34)$$

E. The relevant couplings $\gamma \bar{b}b$ and $Z^0 \bar{b}b$

The other relevant couplings are the gauge bosons with the charged Higgs pair and the $V \bar{b}b$ ($V = \gamma, Z^\mu$) interactions, the former of which are the same as those in SM and the latter are given as[15],

$$\gamma^\mu \bar{b}b : ieQ_b \gamma^\mu, \quad Z^\mu \bar{b}b : \frac{ig}{c_W} [(g_L^b + \frac{1}{4}(s_L^b)^2) - \frac{1}{4}(s_L^b)^2 \gamma^5] \quad (35)$$

F. The simple discussions of the relevant model parameters

Obtaining the relevant couplings, we will now discuss the parameters involved in the models. The parameters of this models related to our discussions are c_1 , c_2 , the mixing angles β , ϕ the scale Λ , the ETC contributions to the masses of the top and the bottom quarks ϵ_t and ϵ_b , the vector-like quark mass m_T and m_B , the scalar masses and the three VEVs of the doublets v_1 , v_2 , v_{TC} , which satisfy $v_1^2 + v_2^2 + v_{TC}^2 = v_{EW}^2$. The vector-like quark mass m_T and m_B are constrained by the oblique parameter and can be chosen as $m_T = m_B = 5$ TeV[15]. The scalar section, the lighter CP-even Higgs are chosen to be the 126 GeV SM-like Higgs, and the charged ones are thought to be heavier than that [15]. Now we simply discuss the constraints of the relevant parameters.

- (1) The compositeness scale Λ is identified with the mass scale of the massive coloron M'_G in the present models. With the constraints of the M'_G [15], $\Lambda > 4$ TeV, a light CP-even Higgs with mass around 126 GeV can be accommodated within the model for arbitrary Λ with $4 < \Lambda < 100$ TeV. To diminish the contributions from the massive topcolor gauge bosons to the electroweak precision parameters at the same time, we here take $\Lambda = 50$ TeV [15].
- (2) The couplings $y_{1,2}$ are solved from RGEs and the compositeness conditions [22, 24]. From Ref. [15], we can see that if the Λ is assumed to be at about 50 TeV, it is suitable to take $y_1 = y_2 = 2$, which will be applied in our discussion.
- (3) About the ϵ_t and ϵ_b parameter, which are the fraction of the ETC contribution to the top and bottom quark masses. Generally, we take this parameter small, $0 < \epsilon_{t,b} < 0.1$, which means that the ETC contribution to the heavy mass is smaller than that of the seesaw section, i.e., the heavy fermion masses are mainly provided by the seesaw mechanism.
- (4) About the mass bounds for the vector-like quarks, in order that fermion sector does not generate a large contribution to the T-parameter, the masses can be set as $m_T = m_B = 5$ TeV [15].
- (5) About the mass bounds for the charged Higgs, of which we will consider the pair production at the LHC, we assume the light ones with a mass larger than 200 GeV, while masses of the heavy ones are in the range from 1000 to 5000 GeV.
- (6) About the mixing angles β, ϕ , which indicate the vacuum structures of the scalars, we will assume they are changing in a certain range, such as $0.5 < \tan \beta, \tan \phi < 10$, $0.5 \leq \tan \phi \leq 10$, which are permitted by the constraints in Ref. [15].

III. THE CHARGED HIGGS PAIR PRODUCTIONS AT THE LHC

In this section, we discuss charged Higgs pair production processes $gg \rightarrow H^+H^-$, $q\bar{q} \rightarrow H^+H^-$ ($q = u, d, s, c, b$), in top-seesaw assisted TC models. In these processes, some couplings such as $H^\pm \bar{f} f'$ ($f, f' = t, b, T, B$) and $SH_L^+ H_L^-$ ($S = h^0, H^0$) etc., contain the

model-dependent parameters so that it may be viable to probe the new physics theory at future collider experiments, via the effects of these parameters.

The cross sections of the charged Higgs pair production at the LHC comes mainly from the gluon gluon fusion $gg \rightarrow H^+H^-$, and quark pair annihilation processes $q\bar{q} \rightarrow H^+H^-$. At the LHC, the parton level cross sections for $pp \rightarrow H^+H^-$ are calculated at the leading order as

$$\hat{\sigma}(\hat{s}) = \int_{\hat{t}_{min}}^{\hat{t}_{max}} \frac{1}{16\pi\hat{s}^2} \overline{\Sigma} |M_{ren}|^2 d\hat{t}, \quad (36)$$

with

$$\hat{t}_{max,min} = \frac{1}{2} \left\{ m_{p_1}^2 + m_{p_2}^2 - \hat{s} \pm \sqrt{[\hat{s} - (m_{p_1} + m_{p_2})^2][\hat{s} - (m_{p_1} - m_{p_2})^2]} \right\}, \quad (37)$$

where p_1 and p_2 are the first and the second initial particles in the parton level, respectively. For our case, they could be gluon g and quarks u, d, c, s, b .

The total hadronic cross section for $pp \rightarrow H_L^+ H_L^- + X$ can be obtained by folding the subprocess cross section $\hat{\sigma}$ with the parton luminosity

$$\sigma(s) = \int_{\tau_0}^1 d\tau \frac{dL}{d\tau} \hat{\sigma}(\hat{s} = s\tau), \quad (38)$$

where $\tau_0 = (m_{p_1} + m_{p_2})^2/s$, and s is the pp center-of-mass energy squared. $dL/d\tau$ is the parton luminosity given by

$$\frac{dL}{d\tau} = \int_{\tau}^1 \frac{dx}{x} [f_{p_1}^p(x, Q) f_{p_2}^p(\tau/x, Q) + (p_1 \leftrightarrow p_2)], \quad (39)$$

where $f_{p_1}^p$ and $f_{p_2}^p$ are the parton p_1 and p_2 distribution functions in a proton, respectively. In our numerical calculation, the CTEQ6L [28] parton distribution function is used and take factorization scale Q and the renormalization scale μ_F as $Q = \mu_F = 2m_H$. The loop integrals are evaluated by the LoopTools package [29].

A. The calculation of the the cross sections of the charged Higgs pair productions at The LHC

In this section, we study cross sections for the double charged Higgs production processes $gg \rightarrow H^+H^-$, $q\bar{q} \rightarrow H^+H^-$. Throughout this paper, we take $m_t = 173$ GeV [30], $\alpha_s(m_Z) = 0.118$ [31] and neglect bottom quark mass.

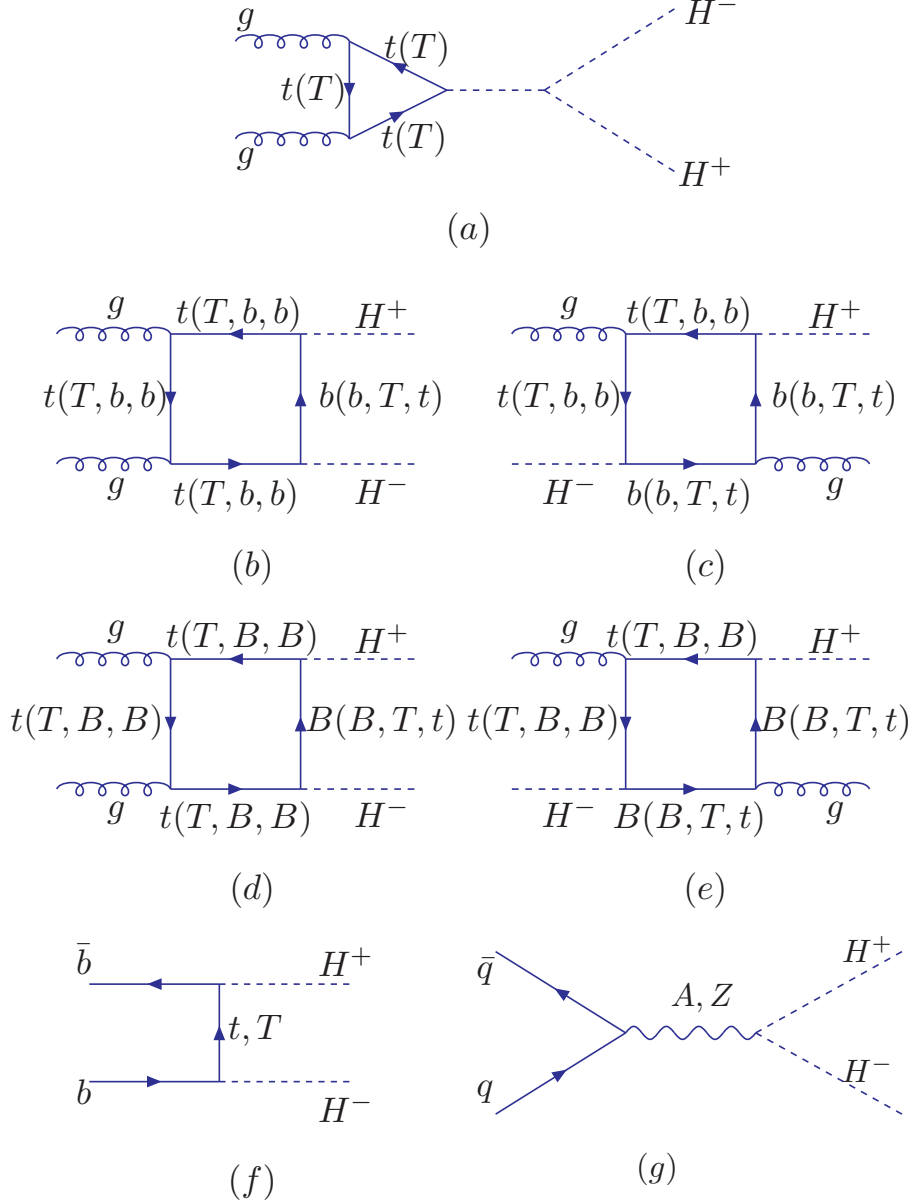


FIG. 1: Feynman diagrams for the charged Higgs pair production at the LHC via gluon fusion and the quark-anti-quark annihilation parton level processes in the top-seesaw assisted TC models are demonstrated, and T , B are the partner quarks of t , b . Those obtained by exchanging the two external gluon lines are not displayed here.

As for the parameters in the present model, we will consider the masses of light Higgs to be 126 GeV, and the masses of the vector-like particle $m_T = m_B = 5$ TeV. Other parameters involved in these processes are the followings: the charged Higgs masses, the mixing of the scalars $\tan \beta$, $\tan \phi$, the dynamical generation quark masses $\Sigma_{U,D}$, and the fraction of the

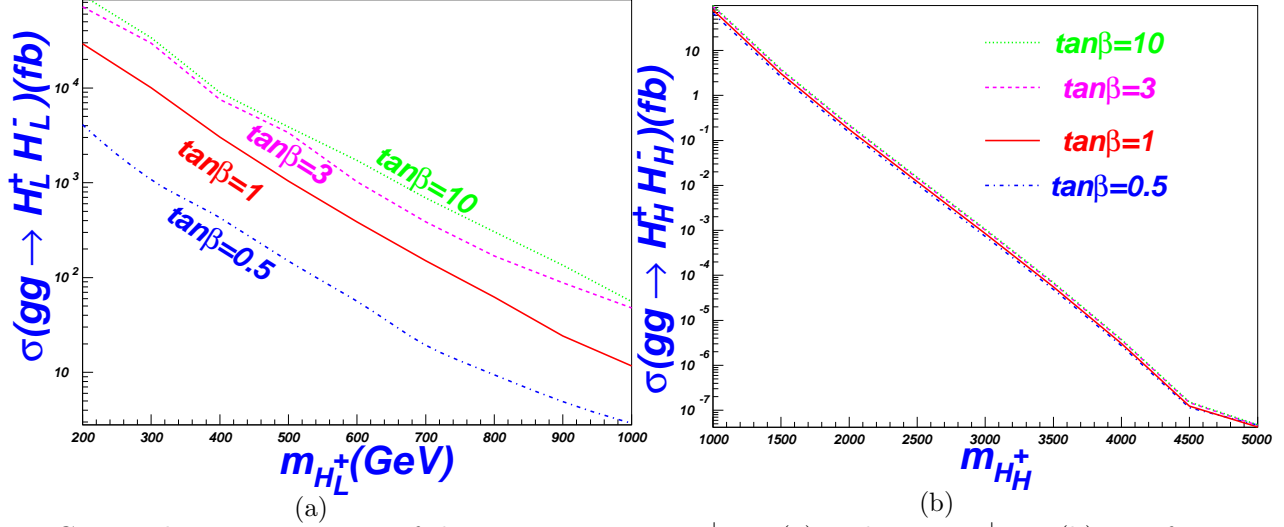


FIG. 2: The cross section σ of the processes $gg \rightarrow H_L^+ H_L^-$ (a) and $gg \rightarrow H_H^+ H_H^-$ (b) as a function of the charged scalar mass m_H with $\tan \beta = 0, 1, 3, 10$ and $\sqrt{s} = 14$ TeV .

ETC sector to the third quark masses, $\epsilon_{t,b}$ parameters. In the following, we will take the light charged Higgs mass m_{H_L} in the range $200 - 1000$ GeV, while the mass of the heavy one mass varies from 1000 to 5000 GeV. Since the parameters Σ_D and ϵ_b are not affected the results largely, we will fix them as $\Sigma_D = 200 \text{ GeV}$ and $\epsilon_b = 0.1$. For other parameters, the ranges can be taken as: $0.5 < \tan \beta < 10$, $0.5 < \tan \phi < 10$, $200 < \Sigma_U \leq 4000$ GeV and $0 \leq \epsilon_t \leq 0.1$.

The parton processes $gg \rightarrow H^+ H^-$, $q\bar{q} \rightarrow H^+ H^-$ ($H^\pm = H_L^\pm, H_H^\pm$) can be produced at the LHC, with the Feynman diagrams shown in Fig.1, which are realized by the gluon fusion and quark-anti-quark annihilation, respectively, so we will firstly discuss the gg fusion and the $q\bar{q}$ annihilation processes, respectively, and then sum them together to obtain the total contributions.

1. The Process $gg \rightarrow H_L^+ H_L^-$ and $gg \rightarrow H_H^+ H_H^-$

Due to the interactions in Eq.(24) and Eq.(30), the charged Higgs pair production processes can be realized by the triangle s-channel and the box t-(u-)channel at the LHC, as shown in Fig.1.

The production cross sections of the $H_L^+ H_L^-$ and $H_H^+ H_H^-$ from the gluon gluon fusion are plotted in Fig.2, for $\sqrt{s} = 14$ TeV, $\tan \phi = 3$, $\epsilon_t = 0.1$, $\Sigma_U = 200$ GeV, and $\tan \beta =$

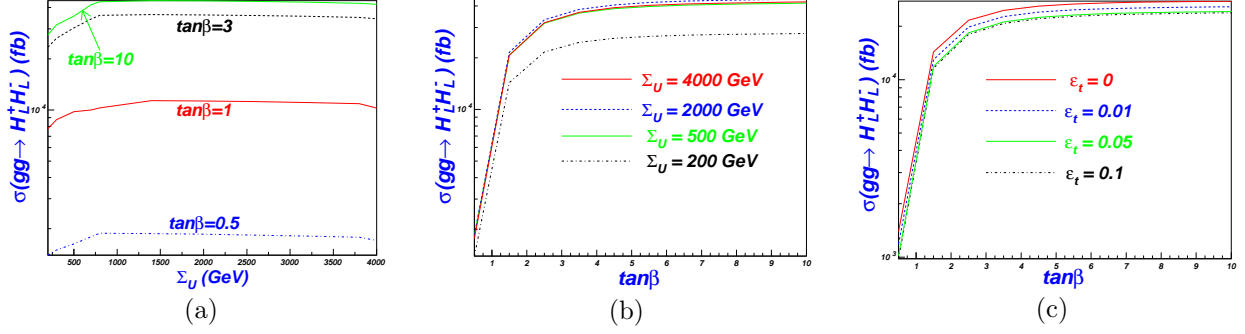


FIG. 3: The cross sections of the processes $gg \rightarrow H_L^+ H_L^-$ are shown, as a function of the dynamical fermion mass Σ_U with $\epsilon_t = 0.1$ and $\tan\beta = 0.5, 1, 3, 10$ (a), and of $\tan\beta$ with $\epsilon_t = 0.1$ and $\Sigma_U = 200, 500, 2000, 4000$ (b), and of $\tan\beta$ with $\Sigma_U = 200$ and $\epsilon_t = 0, 0.01, 0.05, 0.1$ (c), for $\sqrt{s} = 14$ TeV, $m_{H_L} = 300$ GeV and $\tan\phi = 3$.

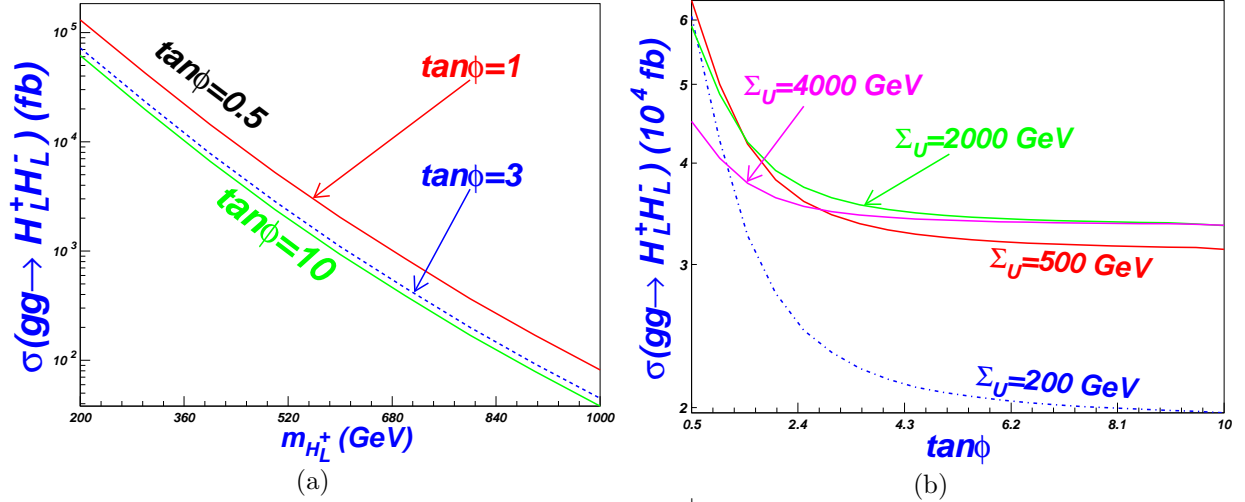


FIG. 4: The cross sections of the processes $gg \rightarrow H_L^+ H_L^-$ are shown, as a function of the charged scalar mass m_{H_L} with $\tan\phi = 0.5, 1, 3, 10$, $\tan\beta = 3$ and $\Sigma_U = 200$ GeV (a), and of $\tan\phi$ with $m_{H_L} = 300$ GeV, $\tan\beta = 3$ and $\Sigma_U = 200, 500, 1000, 2000, 4000$ GeV (b), for $\sqrt{s} = 14$ TeV, and $\epsilon_t = 0.1$.

0, 1, 3, 10, as functions of the charged Higgs mass m_{H_L} and m_{H_H} , with light one changing from 200 to 1000 GeV, and the heavy one from 1000 to 5000 GeV.

From Fig.2, we can see the cross section of this process $H_L^+ H_L^-$ is quite large, which can arrive at 60 pb in a favor parameter space, and in most of the parameter space the cross sections can reach 1 pb only if the charged Higgs is not too heavy. As was expected, the production rate decreases rapidly with the increasing charged Higgs mass since the phase

space are suppressed by the final particle masses, so it is natural that the process $H_H^+ H_H^-$ is smaller than that of the former, about several fbs in most of the parameter space. And with so heavy charged Higgs mass, the suppression was so strong that the varying $\tan \beta$ values are not affected the production rates at all, which shows clearly in Fig.2 (b). In the following, we will only discuss the light charged Higgs pair production unless explicitly stated.

From Fig.2 (a) and Fig.3 (b), we can also see the $\tan \beta$ dependence of the charged Higgs pair production processes is strong, which is understandable, since $\tan \beta$ is closely connected to the scalar VEVs v_1 and v_2 , and the in Fig.1 (a)-(e), the dominant contributions are from the couplings $H^+ t(T) \bar{b}(\bar{B})$ and the three scalars couplings $SH_L^+ H_L^-$ ($S = h^0, H^0$), which are all related directly to the parameter $\tan \beta$.

In Fig.3 (a) we also show the cross sections as the functions of the Σ_U , which is the dynamics fermion mass and find that the production rates are nearly a horizontal line with the varying Σ_U . But in Fig.4 (b), for different Σ_U , the cross sections vary largely, especially, when $\tan \phi$ is large. We can explain this as following: when other parameters contribute large, that from Σ_U is small, but with the increasing $\tan \phi$, the decreasing contributions from ϕ parameter, the effect of Σ_U will stand out. The influence, however, is generally small. So in the following calculation, without affecting the results too much, we will take $\Sigma_U = 200$ GeV.

As for the ϵ_t dependence, we show it in Fig.3 (c) and find the change of the cross sections with the varying ϵ_t are quite limited, so we can conclude that $\epsilon_t = 0.1$ is reasonable in our computation and we will still take as that.

Just as that of the $\tan \beta$, we would like to know how the $\tan \phi$ affects the cross sections. In Fig.4 (a) we give the cross sections varying as the light charged Higgs mass with different $\tan \phi$, and just to find that the effluence of changing $\tan \phi$ are quite small and the curves are almost the same, which is verified by Fig.4 (b), from which we can see that when changing $\tan \phi$ from 0.5 to 10, the curves are almost coincided with each other, especially in the last part of them. Since $v_{TC} = v_{EW} \tan \phi$, we can conclude that the contributions of the TC section are small to the effective couplings $H^+ t \bar{b}$ and $H^0 H_L^+ H_L^-$. Actually, this can be seen clearly from the couplings, for example, the terms closely connected with the $\tan \phi$ in couplings $H^+ t \bar{b}$ can be write out explicitly $(-y_{TC}^b O_{23} + y_{TC}^t O_{23}) + (-y_{TC}^b O_{23} - y_{TC}^t O_{23}) \gamma^5$, and the coefficients $y_{TC} \sim \epsilon_{t,b} < 0.1$, which suppress the contributions; Moreover, the mixing O_{23} decreases largely with the increasing $\tan \beta$, which also suppress the contributions largely.

From the discussion above we can see that the cross sections of the charged Higgs pair production from the gg fusion decline largely with the increasing charged Higgs masses, while, at the same time, the parameters Σ_U , $\tan\beta$, ϵ_t , and $\tan\phi$ will also contribute to the production rates, which increase with the increasing $\tan\beta$ and Σ_U (though very small), and decrease with the increasing $\tan\phi$ and ϵ_t .

We, in this paper, have found a very large rate for the gg fusion production of pair charged Higgs bosons, which seems in contrast with some existing results. For instance, in Ref. [33], for reasonably similar values of the parameters, the cross section of $gg \rightarrow H^+H^-$ is hardly larger than a few fb with the same collider parameters. To explain this clearly, we write down the couplings explicitly. In Ref. [33], the $H^-\bar{t}b$ coupling is $-\frac{1}{\sqrt{2}}[g_t \cot\beta + g_b \tan\beta + (-g_t \cot\beta + g_b \tan\beta)\gamma^5]$ with $g_{t,b} = m_{t,b}/v_{EW}$, and to simplify the discussion, we neglect g_b terms for small m_b , then the coupling can be written as $-g_t/\sqrt{2} \cot\beta(1 - \gamma^5)$, which is inversely proportional to $\tan\beta$. While in our case, the coupling of the $H^-\bar{t}b$ is $(-c_L^t S_R^b O_{21} + s_R^t c_L^b O_{22}) + (-c_L^t S_R^b O_{21} - s_R^t c_L^b O_{22})\gamma^5$ (dismissing the small parts from ETC). and we find that, approximately, it can arrive at $(1 + \gamma_5)$ level in a larger parameter space, since two of the parameters $c_L^{t,b}, S_R^{t,b}$ can be easily close to 1 with large $m_{T,B}$. So the coupling of $H^-\bar{t}b$ is about 3 times larger than that from the that in Ref. [33], with $g_t = 1/\sqrt{2}$ and $\tan\beta = 1.5$. Since there are two $H^-\bar{t}b$ vertexes to the processes, for the cross sections the contributions will be amplified by fourth power, that is, $3^4 = 81$ times larger than that in Ref. [33]. Not to say the large $\tan\beta$, the ratio will be larger(of course, the g_b terms will be large for very large $\tan\beta$). Furthermore, we can see from Fig.1 that the particle spectrum have been added by the third partner particles T, B , which have contributions of almost the same size as the top and the bottom quarks, so the amplitude will be crudely quadrupled and the cross sections will be amplified 16 orders. Thus the total cross sections will be multiplied by a factor $81 \times 16 = 1296$. Of course, this analysis is very crude only as a sketchy estimate. Therefore we conclude that the cross sections in the top-seesaw assisted TC models may be much larger than those in some new physics models.

2. $qq \rightarrow H_L^+ H_L^-$

Here, the $H_L^+ H_L^-$ productions from different parton level have distinct cross sections since the couplings and the parton distribution functions are different, and there is not only

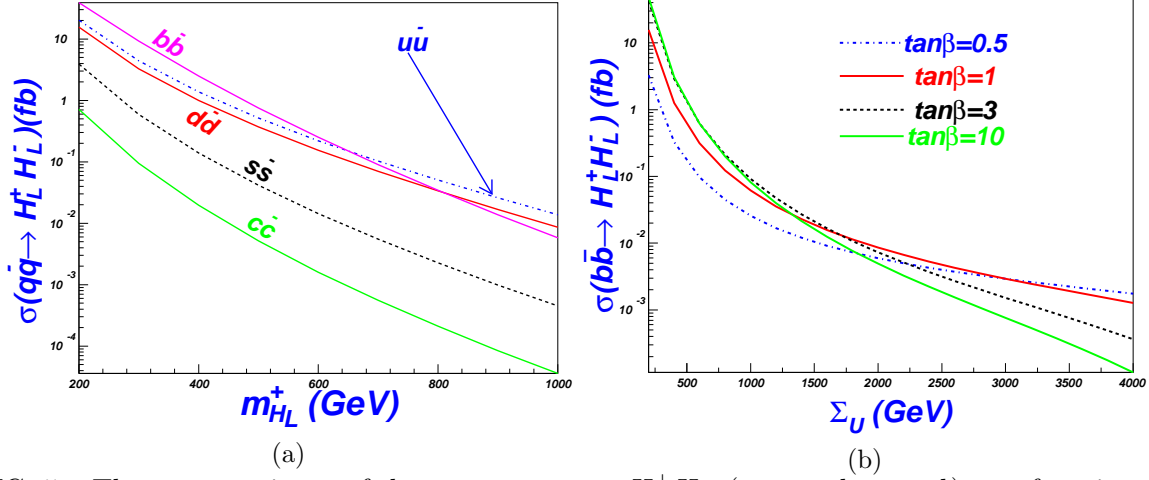


FIG. 5: The cross section σ of the processes $q\bar{q} \rightarrow H_L^+ H_L^-$ ($q = u, d, c, s, b$) as a function of the charged scalar mass m_{H_L} (a) and that of the processes $b\bar{b} \rightarrow H_L^+ H_L^-$ as a function of the parameter ϵ_t (b), respectively, with $\sqrt{s} = 14$ TeV are shown.

s-channel but also t-channel in $b\bar{b} \rightarrow H_L^+ H_L^-$ production, just as shown in Fig.1.

The s-channel processes such as Fig.1 (g), though the parton distribution functions could be larger for the $u\bar{u}$ and $d\bar{d}$ initial state, may be relatively small in view of the center-of-mass suppression effects.

At the same time, the t-channel coupling strengths may be larger than those of the s-channel. In Fig.1 (f), For instance, the strengthen of $H^+ t\bar{b} \sim 1$, which is larger than that of $ZH_L^+ H_L^-$ and $\gamma H_L^+ H_L^-$ (which are about $\sim e$) in the s-channel processes, so the cross sections of the parton level processes like $u\bar{u}(d\bar{d}, s\bar{s}) \rightarrow Z, \gamma \rightarrow H_L^+ H_L^-$ are smaller than those of the others though with larger parton distribution functions. These can be seen clearly in Fig.5.

From Fig.5, we can also see that, in most parameter space, the largest channel of the processes $q\bar{q} \rightarrow H_L^+ H_L^-$ is the $b\bar{b}$ channel, which is easy to understand since, in Fig.1, the t-channel processes (f) are free of the center-of-mass depression and the vertex of $H^+ t\bar{b}$, is in general, larger than that of $ZH_L^+ H_L^-$ and $\gamma H_L^+ H_L^-$, $\sim e$.

We also show the $\tan \beta$ and the Σ_U dependence, respectively, of the cross sections from the $b\bar{b}$ annihilation for $m_{H_L}^+ = 300$ GeV in Fig.5 (b). We can see clearly that the production rates decrease with increasing Σ_U , while for different $\tan \beta$, the production rates do not change much.

Comparing Fig.2, Fig.3 and Fig.4 with Fig.5, we can see that the contributions from gluon fusion is much more important than those from the quark-anti-quark annihilation, and

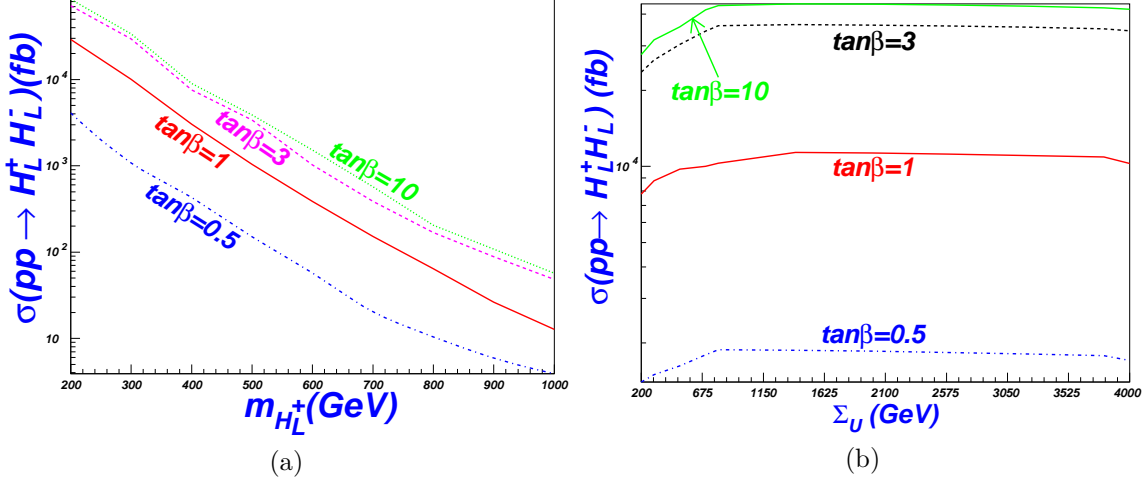


FIG. 6: The total cross sections of the processes $pp \rightarrow H_L^+ H_L^-$ are shown, as a function of the light charged scalar mass m_{H_L} with $\Sigma_U = 200$ GeV (a) and of Σ_U with $m_{H_L} = 300$ GeV (b) for $\sqrt{s} = 14$ TeV, $\epsilon_t = 0.1$.

the former can be about 2 – 3 order larger than the latter.

3. The total contribution for the pair production of the light charged Higgs at the LHC

Here we sum all the contributions, just as shown in Fig.6, from which we can see the total pair production rates of the light charged Higgs are related to the charged Higgs mass and the production probability with $\sqrt{s} = 14$ TeV is larger than 100 fb for $m_H = 600$ GeV in a large parameter space. While, for the good case, for instance, for $m_H = 200$ GeV, the cross section can arrive at several tens pb in most of parameter space.

From Fig.6 and Fig.3, Fig.5, we can see that both the charged Higgs mass and the parameter $\tan \beta$ affects the production rates largely. With different $\tan \beta$, the cross section may be 1 even 2 orders difference, which may be used to constraint this parameter. For example, we can see from Fig.6 (b), with the same parameters, when $\tan \beta = 0.5$ GeV, the cross sections is about 2000 fb, while for $\tan \beta = 10$, the production rate increases to 40000 fb when $m_{H_L} = 300$ GeV.

As for the effect of the parameter Σ_U , the influence is small comparing to that of $\tan \beta$, which can be seen clearly in Fig.6 and Fig.3.

B. Backgrounds Analysis at the LHC

For the light charged Higgs pair production $H_L^+ H_L^-$ at the LHC, the charged light Higgs H^+ decays mainly to $t\bar{b}$, and top quark to b quark, charged lepton and the missing energy, i.e. the $4b + 2l + \cancel{E}$ signal¹ with \cancel{E} , the missing energy, so the mainly SM backgrounds are $pp \rightarrow WWZjj$ (with Z to $b\bar{b}$), $WWZZ$ (with one Z to $b\bar{b}$, the other to jj), $WWhh$, $t\bar{t}W$ (with W to two jets), $WWb\bar{b}jj$ and $t\bar{t}jj$, where h decays to $b\bar{b}$ and the $W \rightarrow l\cancel{E}$. Of course, the signal cross sections would be reduced by the branching ratios, $2/9 \times 2/9 \sim 0.05$ with $Br(W \rightarrow lv) = 2/9$.

The background production rates of the three processes, i.e, $WWZjj$, $WWZZ$ and $WWhh$ are quite small since there are more than 3 QED vertexes which suppress the strength. Considering the branching ratio of W and Z , the cross sections are at the level of several tens of fb, so they are negligible in the SM background discussion. For $pp \rightarrow t\bar{t}W$, the production rate, about 500 fb, similarly, the branching ratio of W decaying to hadrons, $2/3$, $t \rightarrow l\cancel{E}b$, $2/9$, then signal is about 4.6 fb, which is much smaller than that of the signal.

The process $pp \rightarrow WWb\bar{b}jj$, is quite large, about 437 pb, multiplying by the W branching ratios, 21 pb. To suppress it, firstly, we require the transverse momentum cut $p_T^j > 20$ Gev, since in the signal, the transverse momentum of the jets, which are from the light charged Higgs, are large, while the transverse momentum of the jets in the production $pp \rightarrow WWb\bar{b}jj$, are much smaller. So the background will be cut down largely, without losing signatures a lot at the same time. Secondly, the light charged Higgs mass, or the top quark mass reconstruction will be powerful to suppress the background since in the signal the Wb comes from the top quark, and the top quarks are from the charged Higgs, while in the background, it may not be the true case.

Another powerful background is $pp \rightarrow t\bar{t}jj$, about 227pb, including the LO and the NLO contribution[32]. The top quark, however, will decay to Wb with 100% percent, so the process change into a part of the process $pp \rightarrow WWb\bar{b}jj$ and it can also be suppressed by the two methods mentioned above, i.e, the transverse momentum cut and the mass reconstruction.

From the discussion, we believe that the signal of the light charged Higgs will not be

¹ Actually, usually only 2 bottom quarks are tagged, so the signal is $2b + 2l + 2j + \cancel{E}$.

reduced too much, while the background may be suppressed very much. Based on the discussion above, we here arrive at the conclusion that the signal cross sections arriving at 1000 fb may be observable at the LHC. Nevertheless, the discussion here is so crudely, and the precision are far beyond control. We may, in the following work, debate the observability at length.

To draw a very crudely conclusion, for an integrated luminosity 100 fb^{-1} at the LHC, the charged scalar pair production cross sections of 1000 fb may be the lower limit of the observability.

IV. SUMMARY AND CONCLUSION

We considered the charged Higgs pair productions in the top-seesaw assisted TC model, proceeding through $gg \rightarrow H^+H^-$, $q\bar{q} \rightarrow H^+H^-$, as a probe of the model. Since the backgrounds may be effectively suppressed by the scalar mass reconstruction, these processes can be used to probe the model. We found that these charged Higgs pair productions in different collisions can play complementary roles in probing the top-seesaw assisted TC model:

For the heavy charged Higgs pair production at the LHC, the cross section are quite small with the increasing final particle masses, so we will not discuss little about that.

At the LHC, for the light charged scalars, the cross sections are large, and we have discussed the rates at the two parton level, i.e, the gluon gluon fusion and quark-anti-quark annihilation, and compared their relative contribution. We find that the contribution from the former is much larger than that from the latter.

After simple discussion of the backgrounds, for the $H_L^+H_L^-$ production at the LHC, the processes may be detectable when the cross sections reach 1000 fb, as discussed in the above section. For the process $gg \rightarrow H_L^+H_L^-$, the cross section can reach 1000 fb in most of the parameter spaces, which contributes large for this charged production. For $b\bar{b} \rightarrow H_L^+H_L^-$ and $u\bar{u} \rightarrow H_L^+H_L^-$, the cross sections can arrive at several tens of fbs in most of the parameter spaces, which are much smaller than those of the gluon gluon fusion, so the main contribution is from the gluon gluon fusion.

As a conclusion, as long as the charged scalars are not too heavy, e.g., below 600 GeV, the productions might be detectable at the LHC. In general, the light charged Higgs pair productions have larger possibility to be detected since their couplings to $t\bar{b}$ are large. We

see from the figures listed above that in a large part of the parameter space the cross sections of the scalar pair productions can reach the possible detectable level, 1000 fb for the LHC. Therefore, the pair productions of charged Higgs may serve as a good probe of the top-seesaw assisted TC model.

Acknowledgments

This work was supported by the Natural Science Foundation of China under the grant numbers 11105125 and 11105124 and the Excellent Youth Foundation of Zhengzhou U. under the grand number 1421317053.

-
- [1] S. Chatrchyan et al. [CMS Collaboration], Phys. Lett. B 716, 30 (2012); G. Aad et al. [ATLAS Collaboration], Phys. Lett. B 716, 1 (2012).
 - [2] See the web: <http://home.web.cern.ch/topics/large-hadron-collider>.
 - [3] S. L. Glashow, Nucl. Phys. 22, 579 (1961); S. Weinberg, Phys. Rev. Lett. 19, 1264 (1967); A. Salam In Elementary Particle Theory, ed. N. Svartholm (Almquist and Wiksells, Stockholm 1969), 367-377.
 - [4] M. C. Gonzalez-Garcia and Y. Nir, *Rev. Mod. Phys.* **75**, 345(2003); V. Barger, D. Marfatia, and K. Whisnant, *Int. J. Mod. Phys E***12**, 569(2003); A. Y. Smimov, *hep-ph/0402264*.
 - [5] G. Jungman, M. Kamionkowski and K. Griest, Phys. Rept. 267, 195 (1996); G. Bertone, D. Hooper and J. Silk, Phys. Rept. 405, 279 (2005); J. L. Feng, Ann. Rev. Astron. Astrophys. 48, 495 (2010).
 - [6] S. Weinberg, Phys. Rev. D13(1976) 974; *ibid*, D19 (1979) 1277; L. Susskind, Phys. Rev. D20, (1979) 2619; E. Farhi, L. Susskind, Phys.Rept.74,(1981) 277.
 - [7] C. T. Hill, Phys. Lett. B **345**, 483 (1995); K. Lane and E. Eichten, Phys. Lett. B **352**, 383 (1995); K. Lane, Phys. Lett. B **483**, 96 (1998); G. Cvetič, Rev. Mod. Phys. 71, 513 (1999); C. T. Hill and E. H. Simmons, Phys. Rept. **381**, 235 (2003).
 - [8] B. A. Dobrescu and C. T. Hill, Phys. Rev. Lett. **81**, (1998) 2634.
 - [9] R. S. Chivukula, B. A. Dobrescu, H. Georgi, and C. T. Hill, *Phys. Rev. D* **59**, (1999) 075003.
 - [10] B. A. Dobrescu, *Phys. Rev. D* **63**, (2001) 015004.

- [11] H.-J. He, T. Tait, C.-P. Yuan, *Phys. Rev. D* **62**, 011702 (2000).
- [12] H.-J. He, C. T. Hill, and T. M. Tait, *Phys. Rev. D* **65**, (2002) 055006.
- [13] X.-F. Wang, C. Du, H.-J. He, *Phys. Lett. B* **723**, 314 (2013).
- [14] G. Cvetič, *Rev. Mod. Phys.* **71**, 513 (1999); S. P. Martin, *Phys. Rev. D* **46**, 2197 (1992); *Phys. Rev. D* **45**, 4283 (1992), *Nucl. Phys. B* **398**, 359 (1993); M. Lindner and D. Ross, *Nucl. Phys. B* **370**, 30 (1992); R. Bonisch, *Phys. Lett. B* **268**, 394 (1991); C. T. Hill, D. C. Kennedy, T. Onogi, H. L. Yu, *Phys. Rev. D* **47**, 2940 (1993).
- [15] H. S. Fukano, K. Tuominen, *Phys. Rev. D* **85**, (2012) 095025; e-Print: arXiv:1210.6756.
- [16] J. Wess and J. Bagger, "Supersymmetry and supergravity,". Princeton, USA: Univ. Pr. (1992)259 p; S. Gates, M. T. Grisaru, M. Rocek, and W. Siegel, "Superspace Or One Thousand and One Lessons in Supersymmetry," *Front.Phys.* **58** (1983) 1-548, arXiv:hep-th/0108200 [hep-th]; S. Weinberg, "The quantum theory of ?elds. Vol. 3: Supersymmetry,". Cambridge, UK: Univ. Pr. (2000) 419 p; H. Baer and X. Tata, "Weak scale supersymmetry: From super?elds to scattering events,". Cambridge, UK: Univ. Pr. (2006) 537 p; I. J. R. Aitchison, "Supersymmetry in particle physics: An elementary introduction,". SLAC-R-865; P. Binetruy, "Supersymmetry: Theory, experiment and cosmology,". Oxford, UK: Oxford Univ. Pr. (2006) 520 p; M. Drees, "Supersymmetry,". Oxford, UK: Oxford University Press (2007) 536 p; M. Dine, "Supersymmetry and string theory: Beyond the standard model,". Cambridge, UK: Cambridge Univ. Pr. (2007) 515 p; J. Wess, B. Zumino, *Nucl. Phys. B* **70**, (1974) 39.
- [17] N. Arkani-Hamed, A. G. Cohen, T. Gregoire, E. Katz, A. E. Nelson, J. G. Wacker, *JHEP* 0208:021,2002; J. G. Wacker, arXiv:hep-ph/0208235; M. Schmaltz, *Nucl. Phys. Proc. Suppl.* **117** (2003) 40; M. Schmaltz, D. Tucker-Smith, *Ann.Rev.Nucl.Part.Sci.* **55**:229-270,2005.
- [18] Z. Chacko, Hock-Seng Goh, Roni Harnik, *Phys. Rev. Lett.* **96**, (2006) 231802; Z. Chacko, Y. Nomura, M. Papucci, G. Perez, *JHEP* 0601:126,2006, Z. Chacko, H. Goh, R. Harnik, *JHEP* 0601 (2006) 108.
- [19] See e. g., R. Dermisek, J. Hall, E. Lunghi, S. Shin, *JHEP***04**,(2014) 140; Namit Mahajan, *Phys. Rev. D* **90**, 035015 (2014); Xue Gong, Zong-Guo Si, Shuo Yang, Ya-Juan Zheng, *Mod. Phys. Lett. A* **29**, 13 (2014) 1430013; R. Guedes, S. Moretti, R. Santos, *JHEP***1210**, (2012) 119. Guo-Li Liu, Huan-Jun Zhang, Ping Zhou, *JHEP***07**, (2012)081. J. Huang, T. Song, S. Wang, G. Lu, *Chin. Phys. C* **35**, (8) 717 (2011); Qing-Hong Cao, Xia Wan, Xiao-ping Wang, Shou-hua Zhu, *Phys. Rev. D* **87**, (2013) 5, 055022; J. Montalvo, G. Ulloa, M. Tonasse, *Euro.*

- Phys. J. C **72**, (2012) 2210; Shuo Yang, Qi-Shu Yan, JHEP**1202**, (2012) 074; A.G. Akeroyd, Hiroaki Sugiyama, *Phys. Rev. D* **84**, 035010, 2011; A.G. Akeroyd, S. Moretti, *Phys. Rev. D* **84**, (2011) 035028; Guo-Li Liu, Fei Wang, Shuo Yang, *Phys. Rev. D* **88**, 115006 (2013);
- [20] A. Cagil, Nucl. Phys. B **843**, 46 (2011); L. Wang, W. Wang, J. M. Yang, H. Zhang, *Phys. Rev. D* **76**, 017702 (2007); X.-F. Han, L. Wang, J. M. Yang, Nucl. Phys. B **825**, 222 (2010); T. Han, B. Mukhopadhyaya, Z. Si, K. Wang, *Phys. Rev. D* **76**, 075013 (2007); E. Asakawa, E. D. Harada, S. Kanemura, Y. Okada, K. Tsumura, *Phys. Rev. D* **82**, 115002 (2010); A. Gutierrez-Rodriguez, M. Hernandez-Ruiz, O. Sampayo, Int. J. Mod. Phys. A **24**, 5299 (2009); W. Ma, C. X. Yue, Y. Z. Wang, *Phys. Rev. D* **79**, 095010 (2009).
- [21] Y. Nambu and G. Jona-Lasinio, Phys. Rev. **122**, 345 (1961); Phys. Rev. **124**, 246 (1961).
- [22] W. A. Bardeen, C. T. Hill and M. Lindner, *Phys. Rev. D* **41**, 1647 (1990).
- [23] T. Appelquist and C. W. Bernard, *Phys. Rev. D* **22**, 200 (1980); A.C. Longitano, *Phys. Rev. D* **22**, 1166 (1980); Nucl. Phys. B **188**, 118 (1981).
- [24] M. Hashimoto and V. A. Miransky, *Phys. Rev. D* **81**, 055014 (2010).
- [25] R. S. Chivakula, E. H. Simmons, B. Coleppa, H. E. Logan and A. Martin, *Phys. Rev. D* **83**, 055013 (2011).
- [26] Hidenori S. Fukano, Kimmo Tuominen, JHEP**1309**, (2013) 021;
- [27] M. Hashimoto and V. A. Miransky, Phys. Rev. D **81**, 055014 (2010).
- [28] J. Pumplin, et al., JHEP **0207**, 012 (2002).
- [29] T. Hahn and M. Perez-Victoria, Comput. Phys. Commun. **118**, 153 (1999). T. Hahn, PoS ACAT2010, (2010) 078.
- [30] CDF Collaboration, Phys. Rev. Lett. **105**, 252001 (2010).
- [31] Particle Data Group, J. Phys. G **37**, 075021 (2010).
- [32] G. Bevilacqua, et.al, Phys. Rev. Lett. **104**, 162002 (2010).
- [33] A. Krause, T. Plehn, M. Spira, P.M. Zerwas, Nucl. Phys. B **519**, 85 (1998).